Journal of Solid State Chemistry 182 (2009) 289–294

Contents lists available at ScienceDirect

Journal of Solid State Chemistry

journal homepage: www.elsevier.com/locate/jssc

Local environment in $Ba_2In_{2-x}W_xO_{5+3x/2}$ oxide ion conductors

Sylvie Daviero-Minaud, Aurélie Rolle *, Chanapa Kongmark, Rose-Noëlle Vannier

UCCS-Unité de Catalyse et Chimie du Solide, Equipe de Chimie du Solide, ENSCL/UST Lille 1, BP 90 108, 59652 Villeneuve d'Ascq Cedex, France

ARTICLE INFO

Article history:
Received 27 June 2008
Received in revised form
30 September 2008
Accepted 4 October 2008
Available online 22 October 2008

Keywords:
Oxide ion conductors
$Ba_2In_{2-x}W_xO_{5+x/2}$
X-ray absorption spectroscopy

ABSTRACT

The actual oxygen environment of the tungsten dopant in the $Ba_2In_{2-x}W_xO_{5+3x/2}$ solid solution was revealed by combining X-ray absorption spectroscopy at the tungsten L_I and L_{III} edges and at the indium L_I edge. Whatever the substitution ratio, the tungsten atoms exhibit a regular octahedral environment. When the substitution ratio increases, the oxygen vacancies are progressively filled until their total occupancy for $x = 2/3$. For $x \geqslant 0.3$, the perovskite structure is stabilised; the tungsten atoms are randomly distributed in the structure. Although X-ray diffraction revealed a cubic symmetry for these compositions, a local distortion of the indium environment is observed when a tungsten atom is in its surrounding.

1. Introduction

In contrast to diffraction techniques that give a mean view of the long range crystalline structure, X-ray absorption spectroscopy is a powerful technique to characterise the local surrounding of a target element. It is a technique of choice to define the local environment of a dopant in a solid solution, but it may be limited by the small amount of dopant in the structure. It was here applied to tungsten doped $Ba_2In_2O_5$.

$Ba_2In_2O_5$ is known for oxide ion conduction properties above 925 °C [1]. At room temperature, its structure is of Brownmillerite type. It can be described as a defective perovskite composed of alternating "InO" octahedral and tetrahedral layers [2–4]. Its symmetry is orthorhombic. It becomes tetragonal above 925 °C and then cubic at temperature higher than 1040 °C. These two forms are purely oxide ion conductive. With the aim to stabilise at lower temperatures these two high temperature forms, numerous partial substitutions for barium and/or indium atoms have been performed [1–3,5–29]. The possibility of partial substitution for indium with tungsten was first reported by Shimura et al. [19]. It was further confirmed by our group which showed that the $Ba_2In_{2-x}W_xO_{5+3x/2}$ solid solution extends up to the complete filling of the oxygen vacancy of the defect perovskite $x = 2/3$ [20]. The compositions $x = 0.1$ and 0.2 are orthorhombic and tetragonal, respectively. Cubic forms are stabilised for $x \geqslant 0.3$. However, the precise site-occupancy of the dopant (tetrahedral versus octahedral indium sites) and its local surrounding were not examined. This is the aim of this paper.

2. Experimental

$Ba_2In_{2-x}W_xO_{5+3x/2}$ ($0 \leqslant x \leqslant 1$) phases were prepared by solid state route from stoichiometric mixtures of corresponding oxides and carbonates at 1300 °C, with intermediate grindings at 1000 and 1200 °C [20].

The structure of composition $x = 0.1$ was refined at room temperature using X-ray diffraction data, which were collected on a Bruker axs D8 Advance diffractometer equipped with a solX energy dispersive detector in the 10–120° range with a step of 0.02° and a counting time of 35 s per step (Cu$K\alpha = 1.54$ Å). The refinement was carried out using the Fullprof software [30] and its interface WinPLOTR [31]. The Rietveld method was applied.

X-ray absorption spectroscopy was carried out on the BL 11.1 X-ray absorption fine structure (XAFS) line on the Elettra synchrotron in Trieste (Italy), at the tungsten L_I (12100 eV) and L_{III} (10207 eV) edges and at the indium L_I edge (4238 eV). A double Si-crystal (111) monochromator was used to obtain the monochromatic X-ray incident beam. The energy was calibrated with zinc (K edge 9659 eV) and titanium (K edge 4965 eV) metal foils, used as references. The XANES data at the indium L_I edge and at the tungsten L_I and L_{III} edges were collected at room temperature in transmission mode, using ionisation chambers under nitrogen and helium atmospheres. The samples were prepared by filtration of dispersed powder on microporous membranes. An appropriate amount of powder was filtered in function of preliminary calculations performed to avoid signal saturation and to optimise the signal-to-noise ratio. The energy steps and counting times were adjusted to improve the spectra resolution with a 0.2 eV step and an integrating time of 3 s per step near the edges, and a 1 eV step beyond the edges. Each spectrum was treated with the same procedure. The absorption background was linearly extrapolated

* Corresponding author. Fax: +33 320 436 814.
E-mail address: Aurelie.Rolle@ensc-lille.fr (A. Rolle).

0022-4596/$ - see front matter © 2008 Elsevier Inc. All rights reserved.
doi:10.1016/j.jssc.2008.10.011

from E_0 determined at the inflection point of the absorption edge to a value far enough from the absorption edge that coincides with a zero of the EXAFS signal (around 50 eV above the edge). The absorption background was then subtracted and the XANES spectra were normalised.

EXAFS measurements were performed with a 2 eV step and an integrating time of 2 s per step. For each compound, the spectra were accumulated at least three times and then added in order to increase the signal quality. The EXAFS data extraction was performed by standard procedure with the software package EXAFS 1998 developed on Macintosh™ by Michalowicz et al. [32,33]. The ROUND MIDNIGHT software was used to fit EXAFS data with phase shifts and backscattering amplitudes extracted from crystalline references compounds.

3. Results and discussion

With the aim to precisely determine the tungsten atoms environment in the $Ba_2In_{2-x}W_xO_{5+3x/2}$ solid solution (geometry of its environment, number of neighbours and valence), X-ray absorption spectroscopy was carried out at the element edge. Measurements were performed at the tungsten L_I and L_{III} edges and at the indium L_I edge on various tungsten doped compounds. Reference compounds were carefully selected according to the geometrical environment of the studied element. For the tungsten study, phase shifts and backscattering amplitudes were obtained from EXAFS data of $BaWO_4$, in which tungsten atoms have a regular tetrahedral environment with a single distance W–O of 1.78 Å. In order to check that the extracted phases and amplitudes were not dependent on the tetrahedral symmetry and can be used for other environment geometry, refinements were carried out on monoclinic WO_3 and Bi_2WO_6 in which tungsten atoms are in a small-distorted and high-distorted octahedral environment, respectively. In both cases, the calculated distances and the number of neighbours were in good agreement with the crystallographic data. These phases and amplitudes were therefore used for the refinement of the doped compounds.

3.1. X-ray absorption spectroscopy at the tungsten L_I and L_{III} edges

The XANES spectra at the tungsten L_I (12 100 eV) and L_{III} (10 207 eV) edges were performed for tungsten derivatives $Ba_2In_{2-x}W_xO_{5+3x/2}$ with $x = 0.1$ (orthorhombic), $x = 0.2$ (tetragonal), $x = 0.3$ (cubic) and $x = 2/3$ (cubic). In spite of the low substitution ratio (1–5mol%), enough intensity was measured to get transmission spectra of good quality.

The evolution of XANES signal is given in Fig. 1. At the tungsten L_I edge, the XANES spectroscopy provides qualitative information on the site symmetry by studying the existence of the pre-edge, characteristic of the $2s \rightarrow 5d$ transition. $BaWO_4$ exhibits an intense pre-edge, corresponding to $2s \rightarrow 5d$ transitions authorised in a tetrahedral symmetry. This pre-edge is less intense for WO_3 and Bi_2WO_6. Only a small peak is observed because of the octahedral tungsten environment. For the doped compounds, the pre-edge is even less intense. The symmetry of tungsten in the latter is thus higher than in the references and one can conclude that tungsten has a more regular octahedral environment than in Bi_2WO_6 and WO_3. It is worth noticing that the edge position on the XANES spectra of the doped compounds is similar to that of $BaWO_4$, WO_3, Bi_2WO_6 references. This indicates the tungsten has a 6 oxidation state.

A degree 4 polynomial function was used to extract the EXAFS signal $\chi(k)$ obtained at the tungsten L_{III} edge. It was then Fourier transformed with k^2 weight over a Kaiser window considered between 2 and 16.03 $Å^{-1}$. The signal had a weak background at the end of the spectrum, which made possible to take into account the low amplitude oscillations until the end of the spectrum and therefore the whole spectrum was studied here. The evolution of the amplitude of the raw Fourier transform corresponding to the EXAFS signal at the tungsten L_{III} edge for the $Ba_2In_{2-x}W_xO_{5+3x/2}$ compound with $x = 0.3$ is given in Fig. 2. Only one (W–O) sphere is evidenced. The same evolution is observed for the other compositions. The evolution of the amplitude of the filtered Fourier transform corresponding to the EXAFS signal obtained for the first (W–O) sphere of $Ba_2In_{2-x}W_xO_{5+3x/2}$ compounds with $x = 0.1$, 0.2 and 0.3 is plotted in function of the interatomic distance in Fig. 3. Only one neighbours distance around the tungsten atom is evidenced whatever the substitution ratio. The differences between the three studied substitution ratios are very weak and correspond to the experimental error. The EXAFS modulations of this sphere are shown Fig. 4. The structural parameters deduced from the simulation as well as the agreement factors are given Table 1. Whatever the substitution ratio, a good agreement between the experimental and the simulated data is to be noticed. Whatever the substitution ratio, the tungsten atoms of the substituted compounds have six neighbours at a distance of 1.93 Å, with a regular octahedral environment. These results are in perfect agreement with the XANES results obtained at the tungsten L_I edge.

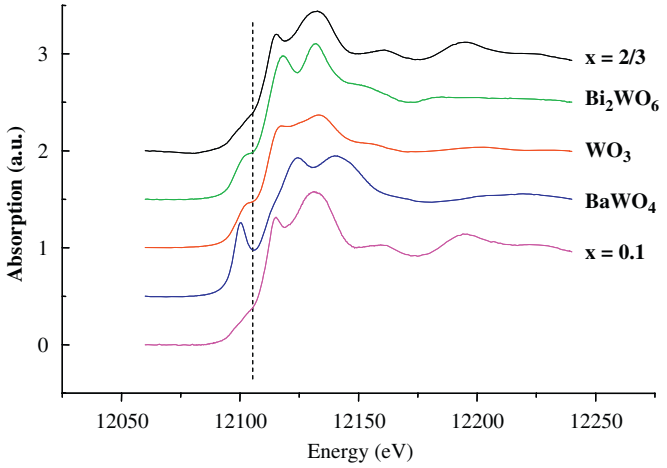

Fig. 1. Evolution of the XANES signal of $Ba_2In_{2-x}W_xO_{5+x}$ type compounds with $x = 0.1$ (orthorhombic), $x = 2/3$ (cubic) and of $BaWO_4$, Bi_2WO_6 and WO_3 references, in which tungsten has a tetrahedral, distorted octahedral and regular octahedral environment, respectively.

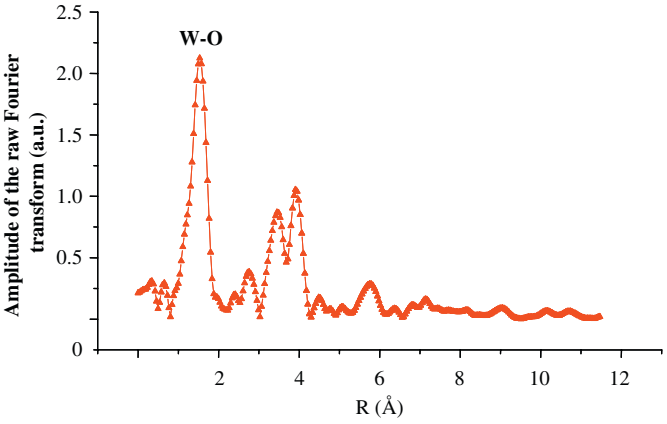

Fig. 2. Raw Fourier transform corresponding to $Ba_2In_{2-x}W_xO_{5+3x/2}$ compound with $x = 0.3$ composition.

3.2. X-ray absorption spectroscopy at the indium L_I edges

It has been reported in the literature [10,24,34] that indium was studied at the *K* edge. However, other studies were undertaken at the *L* edge [35]. In our case, the energy range of the Elettra synchrotron, on which the measurements were performed, allows to reach the energy of the L_I indium edge, only. The XAFS spectra were recorded on the tungsten doped compounds $Ba_2In_{2-x}W_xO_{5+3x/2}$ with $x = 0.1$ (orthorhombic), $x = 0.2$ (tetragonal) and $x = 2/3$ (cubic). $Ba_2In_2O_5$ in which indium has an octahedral and tetrahedral surrounding and In_2O_3 where indium has an irregular octahedral environment were used as crystallised references. Since the edge energy at the indium L_I edge (4238 eV), is very low (soft X-rays) and the air absorption becomes too important, the XAFS spectra were recorded in transmission using a vacuum system. The XANES and EXAFS signals were treated with the procedure described previously.

The atoms located in the near environment of indium are oxygen atoms, whose retrodiffusion amplitude decreases rapidly.

Table 1
Simulation results at the L_{III}-W edge for the tungsten doped compounds with substitution ratio $x = 0.1$, 0.2 and 0.3

Edge	x	Layer i	N_i	σ_i	R_i	ΔE_i	Residue
L_{III}-W	0.1	1	6.12(9)	0.051(9)	1.93(9)	−1(1)	2.5×10^{-3}
L_{III}-W	0.2	1	6.23(8)	0.047(8)	1.93(8)	0.1(8)	3.8×10^{-3}
L_{III}-W	0.3	1	6.4(5)	0.045(8)	1.93(8)	−2.7(8)	6.4×10^{-3}

x: substitution ratio, N_i: number of neighbours, σ_i: Debye–Waller factor, R_i: interatomic distance (Å), ΔE_i: energy difference (eV).

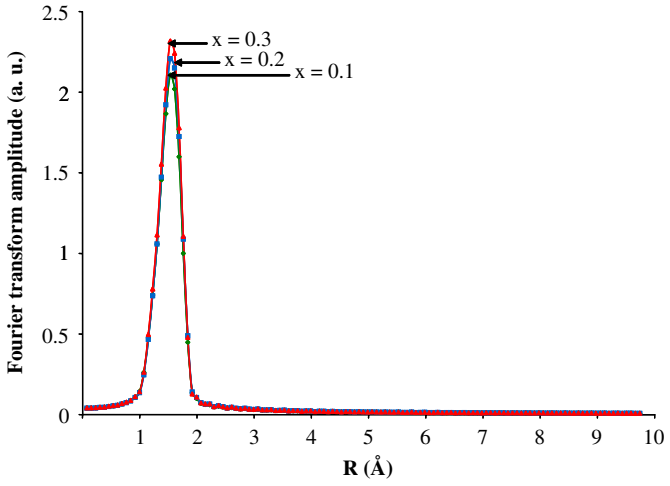

Fig. 3. Fourier transform of EXAFS data at the tungsten L_{III} edge for $Ba_2In_{2-x}W_xO_{5+3x/2}$ doped compounds with $x = 0.1$, 0.2 and 0.3.

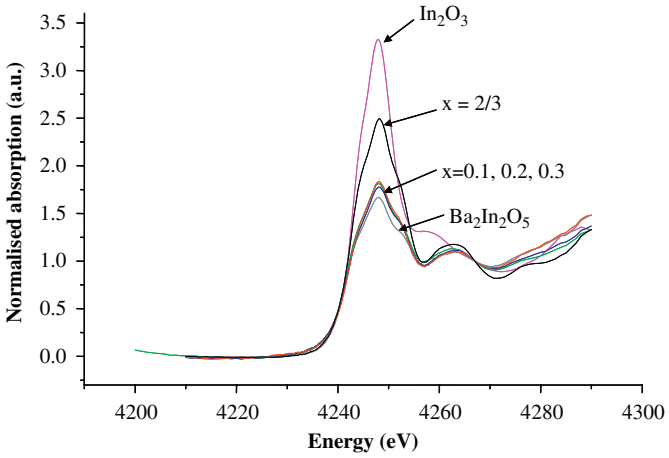

Fig. 5. Evolution of the XANES signal corresponding to $Ba_2In_{2-x}W_xO_{5+3x/2}$ compounds with $x = 0.1$ (orthorhombic), $x = 0.2$ (tetragonal), $x = 0.3$ (cubic), $x = 2/3$ (cubic) and to the references $Ba_2In_2O_5$ (layers of octahedra and tetrahedra) and In_2O_3 (layers of irregular octahedra).

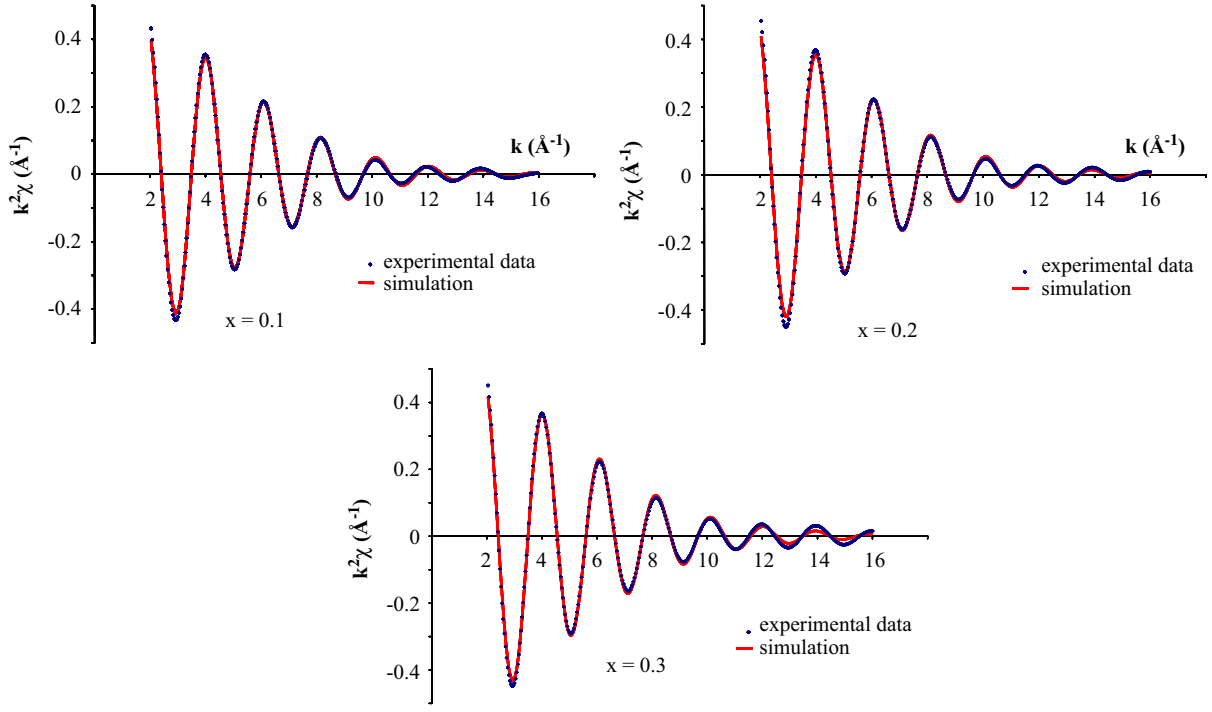

Fig. 4. EXAFS modulations corresponding to the first sphere for tungsten doped compounds with $x = 0.1$, 0.2 and 0.3.

Their contributions to the EXAFS signal at the end of the spectrum are weak and are included in the background. Therefore, the Kaiser window considered for the Fourier transform was limited between 2.39 and 12.70 Å^{-1}. The end of the spectrum was then excluded. Phase shifts and backscattering amplitudes were obtained from EXAFS data of the reference $Ba_2In_2O_5$. In that compound, the octahedral In(1) site is surrounded by six oxygen atoms, including two at 2.31 Å and four at 2.13 Å. The tetrahedral In(2) site is surrounded by four oxygen atoms at a distance of about 2.0 Å [16]. Two experimental phases and amplitudes were obtained by filtering the first sphere at 2.05 Å (average of the short distances: four at 2.13 Å and four at 1.97 Å) and the second at 2.40 Å. For the doped compounds, the two spheres were first fitted separately and then fitted simultaneously.

The XANES spectra recorded at the indium L_I edge are compared in Fig. 5 to those of the reference compounds $Ba_2In_2O_5$ and In_2O_3. This latter consists of layers of irregular octahedra. For small substitution ratios (from $x = 0.1$ to 0.3), the shape of the absorption edge is similar to that observed for $Ba_2In_2O_5$.

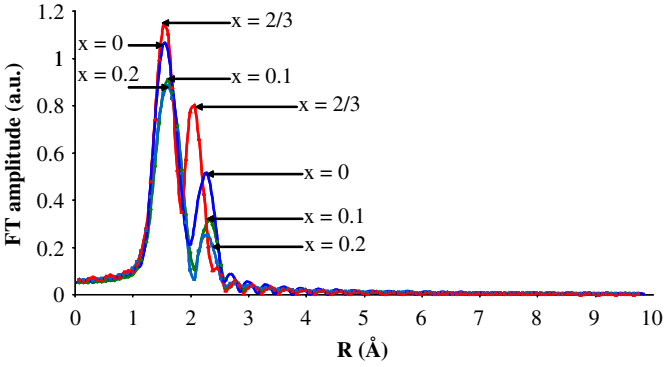

Fig. 6. Fourier transform of the EXAFS signal at the indium L_{III} edge in the case of $Ba_2In_{2-x}W_xO_{5+3x/2}$ type compounds with $x = 0.1$, 0.2 and 2/3.

Its environment is thus equivalent to that of $Ba_2In_2O_5$. When the substitution ratio increases ($x = 2/3$), the edge intensity increases and reaches almost that of the In_2O_3 reference, which consists of layers of irregular octahedra.

The evolution of the Fourier transform amplitude corresponding to the EXAFS signal at the indium L_I edge in function of the interatomic distance in case of $Ba_2In_{2-x}W_xO_{5+3x/2}$ compounds with $x = 0.1$, 0.2 and 2/3 is given in Fig. 6. Two In–O distances are evidenced, but in case of the compound corresponding to the perovskite structure ($x = 2/3$) the second distance is shorter. Fig. 7 shows the corresponding EXAFS modulations. The structural parameters deduced from the simulation and the simulation agreement factors are given in Table 2. The Debye–Waller factors for the $x = 2/3$ composition are typical of ordered compounds and are slightly lower than for the other compositions, which is in agreement with the crystallographic structure of this phase corresponding to a non-oxygen defective perovskite.

In the compounds with substitution ratio $x = 0.1$ and 0.2, indium atoms exhibit two distances, the first one at 2.1 Å and the second one at 2.3 Å. These distances are in agreement with the indium environment in $Ba_2In_2O_5$ with an average of four neighbours at 1.97–2.13 Å and one neighbour at 2.4 Å. In the

Table 2
Simulation results at the L_I-In edge of simulation for the tungsten doped compounds with $x = 0.1$, 0.2 and 2/3

Edge	x	Layer i	N_i	σ_i	R_i	ΔE_i	Residue
L_I-In	0.1	1	4.8(4)	0.06(2)	2.1(2)	1(2)	5×10^{-3}
		2	0.76(2)	0.06(2)	2.3(2)	1(2)	
L_I-In	0.2	1	6(1)	0.08(4)	2.1(2)	1(2)	3×10^{-3}
		2	0.69(8)	0.08(4)	2.3(2)	1(2)	
L_I-In	2/3	1	4.9(3)	0.03(3)	2.1(3)	−2(4)	8×10^{-3}
		2	1.5(3)	0.03(3)	2.1(3)	−2(4)	

x: substitution ratio, N_i: number of neighbours, σ_i: Debye–Waller factor, R_i: interatomic distance (Å), ΔE_i: energy difference (eV).

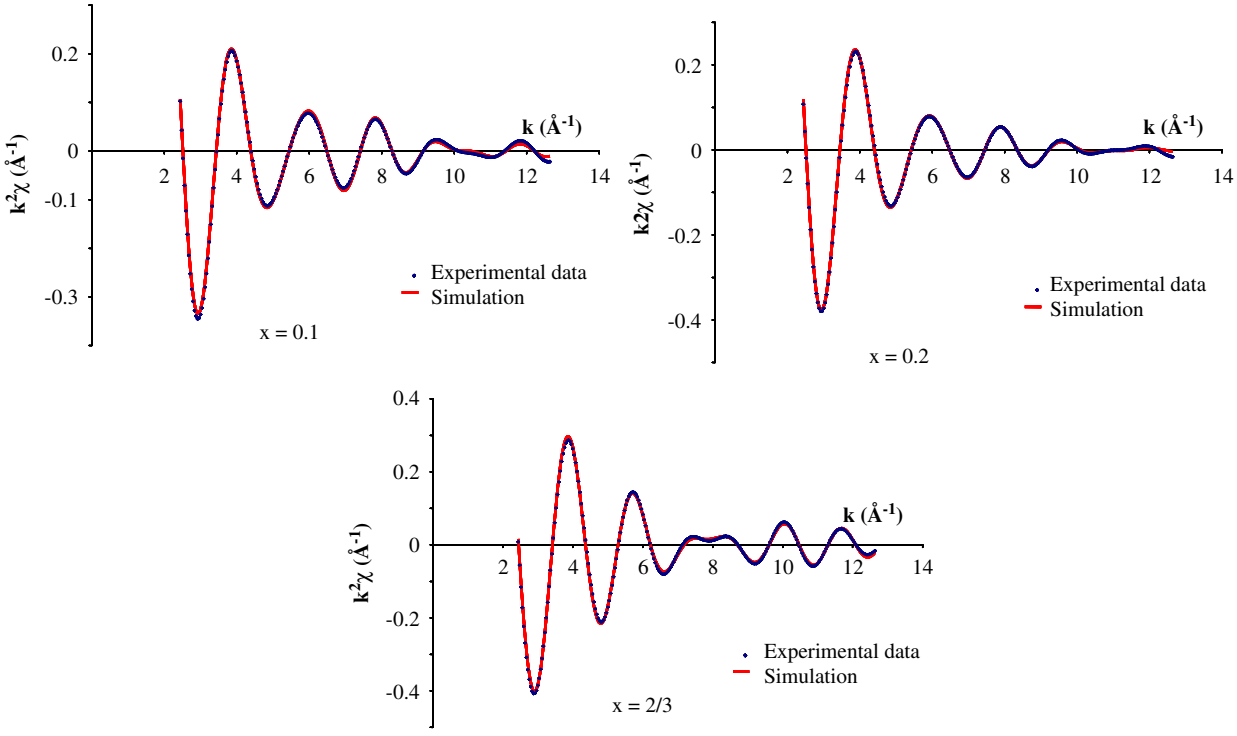

Fig. 7. EXAFS modulations corresponding to the two spheres for the tungsten doped compounds with $x = 0.1$, 0.2 and 2/3.

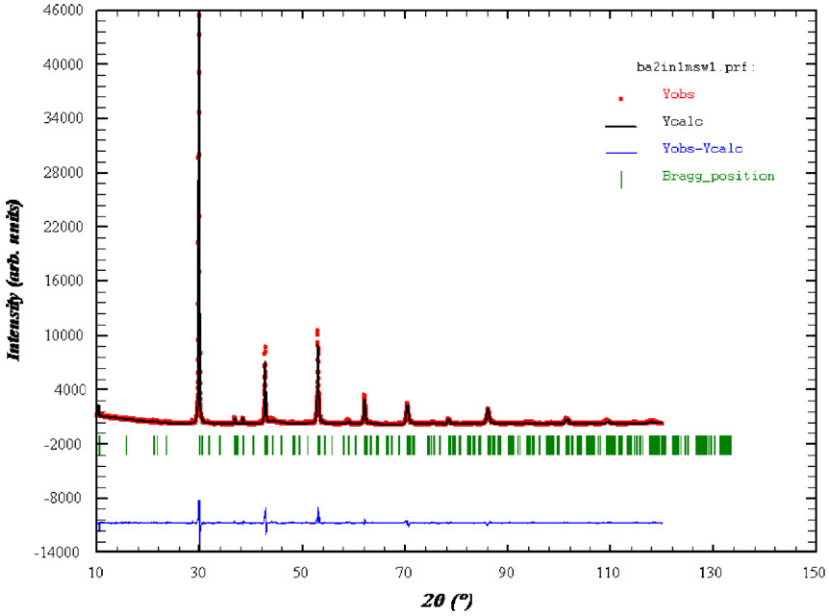

Fig. 8. Calculated diffractogram compared to the experimental data for the $Ba_2In_{1.9}W_{0.1}O_{5.15}$ composition.

substituted compound, the number of neighbours has not been constrained and is higher than in $Ba_2In_2O_5$ with five to six oxygen atoms in the first sphere, but it is associated to a high Debye–Waller factor that explains this overestimated value. In spite of the inaccuracy of the value of the number of neighbours, it is worth noticing that the number of neighbours at 2.1 Å increases from $x = 0.1$ to 0.2 substitution ratios. As a consequence, the fraction of distances at 2.3 Å decreases from $x = 0.1$ to 0.2. The larger Debye–Waller factor shows a more important deformation of the indium site compared to the 2.1 Å sphere in the reference $Ba_2In_2O_5$. The 2.3 Å distance corresponds to the distance of an indium atom with an apical oxygen in the octahedral layers of the Brownmillerite. The decrease in this number would indicate a preferred substitution of indium atom in the octahedral layers. To confirm this assumption, the structure of composition $x = 0.1$ of Brownmillerite-type was tentatively refined from X-ray diffraction data. The structural model proposed by Berastegui [16] for $Ba_2In_2O_5$ in *Icmm* space group was used. As shown in Fig. 8, a good fit between the calculated and experimental data was obtained. But because of the difference of atomic number of W and In ($Z(W) = 74$, $Z(In) = 49$), it was not possible to draw conclusions on the location of W in the structure, indium thermal parameters and reliability factors being almost the same whatever the hypothesis.

For the $x = 2/3$ composition, the refinement of EXAFS data led to five neighbours at 2.1 Å and two neighbours at 2.12 Å. The presence of two types of bonds for a cubic perovskite structure could appear contradictory, but the perovskite structure, evidenced by X-ray diffraction is a mean view of the structure. It corresponds to the superimposition of several environments for the indium atom. With two long bonds and four short bonds, one could conclude to a distorted octahedral environment for the indium atom. It is most probably the superimposition of several types of octahedra with 1/3 of bonds at 2.15 Å and 2/3 at 2.05 Å in average. As shown before, tungsten exhibits a regular octahedral environment with a shorter distance W–O of 1.93 Å. The $x = 2/3$ composition corresponds to 1/3 of indium atoms replaced by tungsten atoms. One can therefore conclude that the 1/3 of the In–O bonds at a distance of 2.15 Å correspond to In–O–W configurations. No superstructure or diffusion lines were evidenced by electronic diffraction. Thus, one can conclude that, in the cubic form, the tungsten atoms in regular octahedral environment are randomly distributed in the structure, which disturbs locally the indium environment which exhibits a longer In–O bond length when a tungsten atom is in the indium surrounding.

4. Conclusions

Whereas X-ray diffraction provides mean information on the average structure, EXAFS and XANES have proven to be local probes to define the accurate surrounding of the W dopant and its location in the $Ba_2In_{2-x}W_xO_{5+3x/2}$ solid solution. It revealed a regular octahedral environment with a W–O distance of 1.93 Å, whatever the substitution ratio. For small substitution ratios (from $x = 0.1$ to 0.3), the shape of the absorption edge at the indium L_I edge is similar to that observed for $Ba_2In_2O_5$. A small decrease in the number of the 2.3 Å In–O distance from $x = 0.1$ to 0.2 could indicate a decrease in the number of indium atom in octahedral layers of the Brownmillerite structure. But, because of the inaccuracy of this number, it is difficult to conclude on the actual location of tungsten atoms in the Brownmillerite structure. Then, for higher substitution ratio, the filling of the vacancies occurs progressively until the total occupation, which leads to the non-oxygen defective perovskite at $x = 2/3$. For $x \geqslant 0.3$, the perovskite structure is stabilised with tungsten atom randomly distributed in the structure. However, although X-ray diffraction revealed cubic symmetry for these compositions, a local distortion of the indium environment is observed when a tungsten atom is in its neighbourhood. Because of the presence of shorter W–O bonds, the In–O bonds are locally longer in the tungsten atoms surroundings.

Acknowledgments

Dr. Belin (local contact on an EXAFS line—ex Lure, Soleil, France) and Dr. Olivi (local contact on an EXAFS line—Elettra, Trieste, Italy) are gratefully acknowledged for their help and

availability during the experiment at Elletra. L. Burylo and M. Huvé are acknowledged for X-ray diffraction and TEM, respectively. The Fonds Européen de Développement Régional (FEDER), the Centre National de la Recherche Scientifique (CNRS), the Région Nord Pas-de-Calais and the Ministère de l'Education Nationale, de l'Enseignement Supérieure et de la Recherche are acknowledged for fundings of X-ray diffractometers. A.R. is grateful to the CNRS and the Région Nord Pas-de-Calais for the funding of her Ph.D. grant.

References

[1] J.B. Goodenough, J.E. Ruiz-Diaz, Y.S. Zhen, Solid State Ionics 44 (1990) 21.
[2] D.H. Gregory, M.T. Weller, J. Solid State Chem. 107 (1) (1993) 134.
[3] S.B. Adler, J.A. Reimer, J. Baltisberger, U. Werner, J. Am. Chem. Soc. 116 (1994) 675.
[4] S.A. Speakman, J.W. Richardson, B.J. Mitchell, S.T. Misture, Solid State Ionics 149 (2002) 247.
[5] S. Kambe, I. Shime, S. Ohshima, K. Okuyama, N. Ohnishi, K. Hiraga, Physica C 220 (1994) 119.
[6] A.L. Kharlanov, N.R. Khasanova, M.V. Paromova, E.V. Antipov, L.N. Lykova, L.M. Kovba Russ., J. Inorg. Chem. 35 (12) (1990) 1741.
[7] C.A.J. Fisher, B. Derby, R.J. Brook, Br. Ceram. Proc. 56 (1996) 25.
[8] H. Yamamura, Y. Yamada, T. Mori, T. Atake, Solid State Ionics 108 (1998) 377.
[9] H. Yamamura, H. Hamazaki, K. Kakinuma, T. Mori, H. Haneda, J. Korean Phys. Soc. 35 (1999) 200.
[10] T. Yao, Y. Uchimoto, M. Kinuhata, T. Inagaki, H. Yoshida, Solid State Ionics 132 (2000) 189.
[11] K. Kakinuma, H. Yamamura, T. Atake, J. Therm. Anal. Calorim. 69 (2002) 897.
[12] A. Yamaji, K. Kawakami, M. Arai, T. Adachi, Mater. Res. Soc. Symp. 575 (2000) 343.
[13] K.R. Kendall, C. Navas, J.K. Thomas, H.C. zur Loye, Solid State Ionics 82 (1995) 215.
[14] A. Manthiram, J.F. Kuo, J.B. Goodenough, Solid State Ionics 62 (1993) 225.
[15] J.B. Goodenough, A. Manthiram, J.F. Kuo Mater., Chem. Phys. 35 (1993) 221.
[16] P. Berastegui, S. Hull, J. Garcia-Garcia, S.G. Eriksson, J. Solid State Chem. 164 (2002) 119.
[17] V. Jayaraman, A. Magrez, M. Caldes, O. Joubert, M. Ganne, Y. Piffard, L. Brohan, Solid State Ionics 170 (1–2) (2004) 17.
[18] T. Schober, Solid State Ionics 109 (1998) 1.
[19] T. Shimura, T. Yogo, Solid State Ionics 175 (2004) 345.
[20] A. Rolle, N.V. Giridharan, R.N. Vannier, F. Abraham, Solid State Ionics 176 (2005) 2095.
[21] M. Yoshinaga, M. Yamaguchi, T. Furuya, S. Wang, T. Hashimoto, Solid State Ionics 169 (2004) 9.
[22] K. Kakinuma, H. Yamamura, H. Haneda, T. Atake, Solid State Ionics 154–155 (2002) 571.
[23] K. Kakinuma, H. Yamamura, H. Haneda, T. Atake, J. Therm. Anal. Calorim. 57 (1999) 737.
[24] Y. Uchimoto, T. Yao, H. Takagi, T. Inagaki, H. Yoshida, Electrochemistry 68 (2000) 531.
[25] K. Kakinuma, H. Yamamura, H. Haneda, T. Atake, Solid State Ionics 140 (2001) 301.
[26] Y. Liu, R.L. Withers, J.F. Gerald, J. Solid State Chem. 170 (2003) 247.
[27] K. Kakinuma, N. Takahashi, H. Yamamura, K. Nomura, T. Atake, Solid State Ionics 168 (2004) 69.
[28] J.B. Goodenough, Solid State Ionics 94 (1997) 17.
[29] H. Kuramochi, T. Mori, H. Yamamura, H. Kobayashi, T. Mitamura, J. Ceramic Soc. Jpn. 102 (1994) 1160.
[30] T. Roisnel, J. Rodriguez-Carvajal, Physica B 192 (1993) 55 See also 〈http://www-llb.cea.fr/fullweb/ftp2k/ftp2k.htm〉.
[31] T. Roisnel, J. Rodriguez-Carvajal, WinPLOTR: a Windows tool for powder diffraction patterns analysis, in: R. Delhez, E.J. Mittenmeijer (Eds.), Proceedings of the 7th European Powder Diffraction Conference (EPDIC7), Materials Science Forum, Trans Tech Publications Ltd., Switzerland, 2000, p. 118, see also 〈http://www-llb.cea.fr/fullweb/winplotr/winplotr.htm〉.
[32] A. Michalowicz, V. Noinville, EXAFS pour le M0AC, Société Française de Chimie, Paris, 1991, p. 102.
[33] A. Michalowicz, J. Phys. IV C2 (1997) 235.
[34] Y. Uchimoto, M. Kinuhata, T. Yao, EXAFS study of coordination structures of Gd-doped $Ba_2In_2O_5$, Jpn. J. Appl. Phys. 38 (Suppl. 1) (1999) 111–114.
[35] M. Womes, J.C. Jumas, J. Olivier-Fourcade, Solid State Commun. 131 (2004) 257.